STABILIZATION OF DOMINANT STRUCTURES IN AN IONIC REACTION–DIFFUSION SYSTEM

Roland KRAMER[1] and Arno F. MUNSTER[2,]*

Institute of Physical Chemistry, University of Wurzburg, Am Hubland, D-97074 Wurzburg, Germany; e-mail: [1] roland.kraemer@sap-ag.de, [2] phch030@phys-chemie.uni-wuerzburg.de

Received December 10, 1997
Accepted April 15, 1998

We describe a method of stabilizing the dominant structure in a chaotic reaction–diffusion system, where the underlying nonlinear dynamics needs not to be known. The dominant mode is identified by the Karhunen–Loeve decomposition, also known as orthogonal decomposition. Using a ionic version of the Brusselator model in a spatially one-dimensional system, our control strategy is based on perturbations derived from the amplitude function of the dominant spatial mode. The perturbation is used in two different ways: A global perturbation is realized by forcing an electric current through the one-dimensional system, whereas the local perturbation is performed by modulating concentrations of the autocatalyst at the boundaries. Only the global method enhances the contribution of the dominant mode to the total fluctuation energy. On the other hand, the local method leads to simple bulk oscillation of the entire system.
Key words: Control of chaos; Orthogonal decomposition; Spatiotemporal patterns.

The control of chaotic behaviour of nonlinear dynamical systems by systematic perturbations has been extensively studied during recent years. Significant progress has been made in controlling chaos in homogeneous systems with few degrees of freedom. Small and carefully chosen perturbations of an arbitrary parameter of the system can confine the dynamics close to a desired unstable fixed point or unstable periodic orbit. This so-called OGY method has been successively tested in a number of experiments[1–3]. Besides the discontinuous OGY method a continuous way of chaos control based on time-delayed feedback was introduced by Pyragas[4–6]. A common feature of both mentioned methods is that the perturbation almost decreases to zero when the target dynamics are achieved. Recently a resonant perturbation of chaos was proposed by Schneider *et al.*[7]. These authors used the dominant frequency of a chaotic time series for harmonically modulating the flow rate through a stirred reactor and observed the same periodic orbits which resulted from a control by the Pyragas method. A sinusoidal

* The author to whom correspondence should be addressed.

perturbation was also applied to the gas flow in the chaotic CO oxidation. In this case a periodically oscillating CO_2 concentration was obtained; this was interpreted, however, not in the sense of a stabilized unstable orbit[8].

Control of chaos in distributed systems generally cannnot be achieved by using a single measurement $X(t)$ at one chosen location and linking it with a lumped input variable *via* a linear control law of the OGY or Pyragas type. These methods cannot be applied to spatially extended systems if the correlation length of the spatio-temporally chaotic pattern is smaller than the size of the system. Taking a set of grid points inside a spatially one-dimensional system into account, a proper controlling perturbation may be computed by the projection of the measured output variable onto a desired target dynamics, which can be determined by Karhunen–Loeve (KL) decomposition[9–11]. In this paper we demonstrate the control of spatiotemporal chaos in a simple, spatially one-dimensional reaction–diffusion–migration system.

THE MODEL

For a description of nonlinear chemical kinetics, we used a ionic version of the well-known Brusselator[12] which is described by the following reaction scheme.

$$\begin{aligned} A &\rightarrow X^+ + C^- \\ B + X^+ &\rightarrow Y^+ + D \\ 2\,X^+ + Y^+ &\rightarrow 3\,X^+ \\ X^+ &\rightarrow X^{*+} \\ X^{*+} + C^- &\rightarrow E \end{aligned} \qquad (1)$$

All reactions are assumed to be irreversible, the last reaction step being fast compared to the others and the educts A and B are assumed to be present in excess. Their concentrations therefore are treated as constant parameters of the model. Anion C serves to balance the charges of the activator X and the inhibiting species Y. This modified ionic Brusselator scheme is described in detail elsewhere[12]; there, also the scaling of all dimensionless variables and parameters is given. Using the Nernst–Planck equation to express the fluxes of the essential compounds, the model results in the following dimensionless mass balance equations:

$$\begin{aligned} \frac{\partial X}{\partial \tau} &= -\nabla\,(-D_X \nabla X - D_X X\,\nabla\varphi) + A - (B+1)X + X^2 Y \\ \frac{\partial Y}{\partial \tau} &= -\nabla\,(-D_Y \nabla Y - D_Y Y\,\nabla\varphi) + BX - X^2 Y \\ \frac{\partial C}{\partial \tau} &= -\nabla\,(-D_C \nabla C + D_C C\,\nabla\varphi) + A - X\ , \end{aligned} \qquad (2)$$

where X, Y, *etc*. are dimensionless concentrations of species X, Y, *etc*., D_i are dimensionless diffusion coefficients, and φ stands for the appropriately normalized electric potential.

The mass balance of C may be expressed from the balances of X and Y using the (approximate) local electroneutrality assumption. As pointed out in previous work[12], an expression for the self-consistent electric field may be derived in a spatially one-dimensional system. For the local gradient of the electric potential inside the reaction–diffusion–migration system one finds:

$$-\nabla\varphi = \frac{I + (D_\mathrm{X} - D_\mathrm{C})\nabla X + (D_\mathrm{Y} - D_\mathrm{C})\nabla Y}{(D_\mathrm{X} + D_\mathrm{C})\, X + (D_\mathrm{Y} + D_\mathrm{C)}\, Y} \quad . \tag{3}$$

Here the appropriately normalized electric current I flowing through the medium is spatially uniform throughout the system and it is considered as a tunable parameter.

RESULTS AND DISCUSSION

It is well known that spatiotemporal oscillations emerge in the classical Brusselator for proper values of A and B if the diffusion constant of the activator is equal or larger than the diffusion constant of the inhibitor. In our computations with the dimensionless parameter set ($A = 2$, $B = 5.4$, $D_\mathrm{X} = 0.008$, $D_\mathrm{Y} = 0.004$, $D_\mathrm{C} = 1.0$) the diffusion constant of the activator X was chosen to be twice the diffusivity of the inhibitor Y. Under these conditions, the modified ionic Brusselator displays a sequence of periodic, quasiperiodic and irregular oscillatory states depending on the system length. Similar behaviour in the classical Brusselator has been reported a decade ago[13,14]. Our goal in the present work, however, was to control the spatiotemporal chaos as demonstrated below.

At system lengths below $L = 4.99$ (dimensionless units[12]) the entire system oscillates in phase with a simple period one. If the system length exceeds this value, a quasiperiodic regime is found. Here an amplitude defect embedded in the oscillatory background develops. This defect slowly travels back and forth through the system thus reflecting the second frequency of an underlying torus. In an interval between $L = 5.1$ and $L = 7.8$, in-phase oscillations of period one appear again. At system lengths beyond $L = 7.8$, chaotic regimes interrupted by period one states are found. In the chaotic states, amplitude defects move through the system in an irregular fashion while the background still oscillates in a relatively periodic way. An example of spatiotemporal chaos in the ionic Brusselator is depicted in Fig. 1a.

In order to control the spatiotemporal dynamics described above, we followed the strategy of modal feedback control[11,15,16]. A natural choice of modes suitable for control is to make use of orthogonal modes derived from the Karhunen–Loeve decomposition. In the KL decomposition, the spatiotemporal pattern made up by a representative system variable $X(x,t)$ is decomposed into orthogonal spatial functions $\Phi(x)$ (called *topos*) and time-dependent amplitude coefficients $a(t)$ (*chronos*) according to

$$X(x,t) = \sum_{i=1}^{M} a_i(t)\ \Phi(x)\ . \qquad (4)$$

Here M denotes the number of equally-spaced grid points employed to discretize the spatial coordinate x of total length L. The spatial basis functions are computed from the eigenvectors of the auto-covariance matrix $R(x,x')$ which is approximated numerically by the expression

$$R(x,x') = \frac{1}{M} \sum_{i=1}^{M} X_i(x)\ X_i(x')\ .$$

The amplitude functions are obtained by projecting the basis functions onto the original pattern

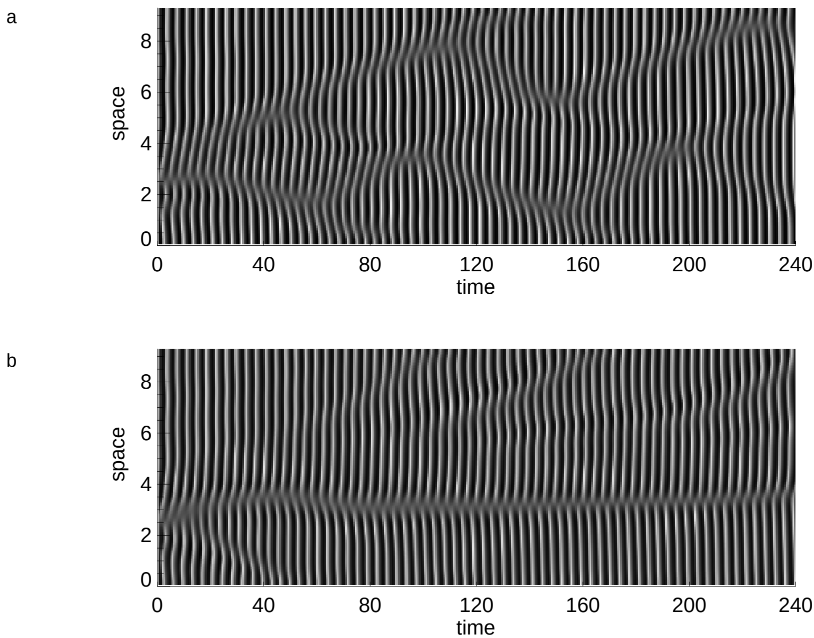

FIG. 1
Space–time plots of the autocatalytic variable X (dimensionless) without control (a) and with control by an electrical field (b). The scale of grey levels encodes the interval between 0.0 (white) and 4.0 (black) dimensionless units of X

$$a_i(t) = (X(x,t),\Phi_i(x)) \ , \tag{6}$$

where (... , ...) denotes the inner product on the space coordinate x. Only the fluctuating part of the signal is considered, *i.e.*, the time average $\langle X(x) \rangle$ is subtracted at each grid point before the decomposition is performed.

Once the dominant structure (mode) $\Phi_d(x)$ has been identified, a proper control parameter P is modulated according to

$$P(t) = P_0(X(x,t),\Phi_d(x)) = P_0 a_d(t) \ , \tag{7}$$

where P_0 is the unperturbed value of parameter P and $a_d(t)$ is the amplitude (*chronos*) of the dominant mode at the actual time t. In the computations presented here, we chose the electric current driven through the system and the boundary values of the autocatalytic variable X as control parameters; the concentration profiles of the activator X were also used in the KL decomposition. The electric current driven through the one-dimensional system thus was modulated according to

$$I(t) = I_0(X(x,t),\Phi_d(x)) = I_0 \ a_d(t) \ . \tag{8}$$

It follows from charge conservation in chemical reactions that current I in the ionic Brusselator in one-space dimension must be spatially uniform and thus it represents a tunable parameter of the system. Furthermore, current perturbations act upon the entire system at the same time and represent a way of globally perturbing the dynamics. In Fig. 1b, a space–time density plot of variable X under chaos control by current modulations is depicted. Here we modulated the current driven through the system according to Eq. (*8*) at a value of the unperturbed current I_0 = 3.8. An amplitude defect is locally pinned by feedback perturbations and the oscillations within the system are fairly regular. In Fig. 2, the dominant KL modes of the uncontrolled chaotic and the controlled state are shown. Furthermore, Fig. 3 shows the relative energy captured by the three most important KL modes as a function of the control amplitude I_0. From the figures it can be seen that the control has stabilized a spatial mode which is similar to the leading mode of the chaotic state. The energy captured by the dominant mode is maximal for a control amplitude of I_0 = 3.8, where the leading mode contributes 55% to the total fluctuation energy. In other words, the number of degrees of freedom required to construct a satisfactory approximation of the spatiotemporal behavior is minimal in that case. The corresponding amplitude functions are aperiodic in the case of chaotic behavior (Fig. 4) but are fairly periodic with amplitude variations less than 10% in the controlled case.

On the basis of the KL decomposition, one may compute space- and time-dependent entropy-like functions which measure the temporal complexity at each spatial grid point and the time-averaged spatial complexity of the system, respectively[17,18]. These entropies are defined by

$$H_s(t) = -\frac{1}{\log N} \sum_{i=1}^{N} p_{ai}(t) \log p_{ai}(t)$$

$$H_t(x) = -\frac{1}{\log N} \sum_{i=1}^{N} p_{\Phi i}(x) \log p_{\Phi i}(x) \quad , \tag{9}$$

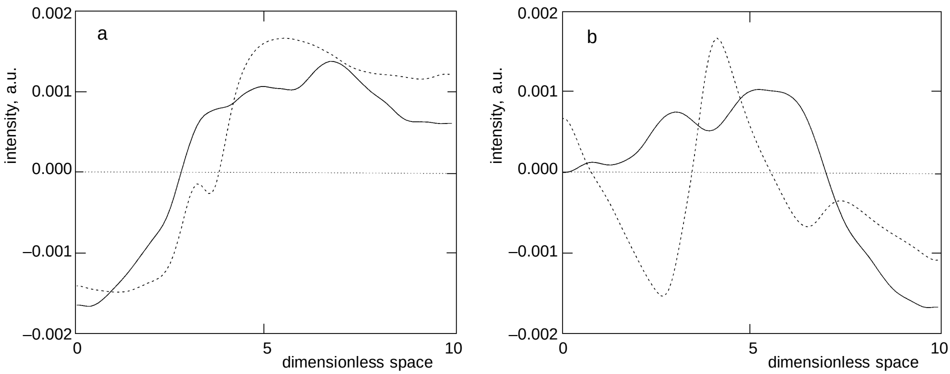

FIG. 2
First (a) and second (b) KL mode with control (dashed line) and in the free running chaotic system

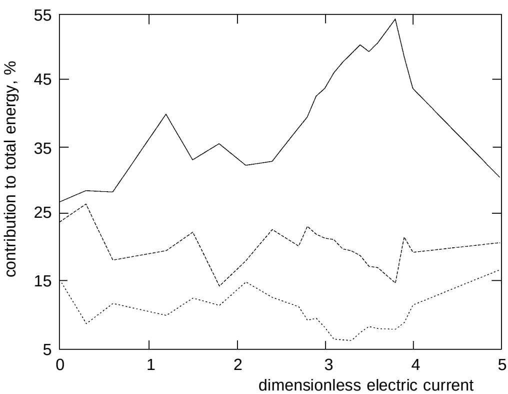

FIG. 3
Contribution of the first three spatial modes to the total fluctuation energy in dependence on electric current I_0

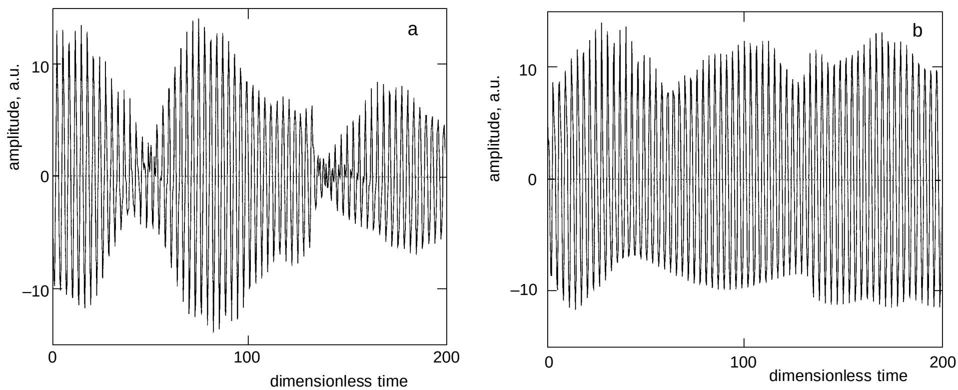

FIG. 4
Time series of the first KL amplitude computed for the same time interval and from the same initial conditions. Unperturbed system (a); controlled system with $I_0 = 3.8$ (b)

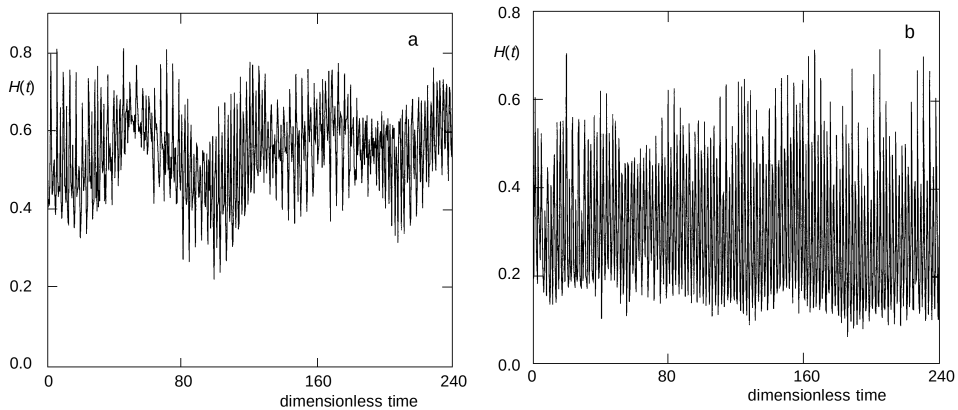

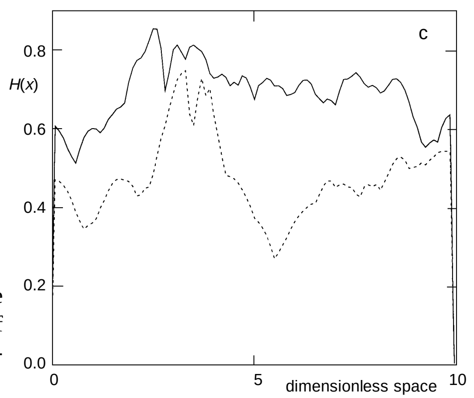

FIG. 5
Temporal entropies $H(t)$ of the chaotic (a) and the controlled (b) system. c Spatial entropy $H(x)$ of the chaotic (solid line) and the system under control (dashed line)

where the probabilities are given by the expressions

$$p_{ai}(t) = \frac{\lambda_i\,|a_i(t)|}{\sum_{j=1}^{N} \lambda_j\,|a_j(t)|}$$

$$p_{\Phi i}(x) = \frac{\lambda_i\,|\Phi_i(x)|}{\sum_{j=1}^{N} \lambda_j\,|\Phi_j(x)|} \quad . \qquad (10)$$

Here, λ is an eigenvalue of the auto-covariance matrix. The temporal and spatial entropies for the uncontrolled system and the system under control are depicted in Fig. 5. It is clearly seen that the complexity of the system dynamics is reduced by the modulated electric current. The entropy, however, remains non-zero in the controlled case corresponding to the relatively complex, but almost periodic spatiotemporal oscillations which cannot be described by a single KL mode.

In order to compare the control by global parameter modulation with a local control of the boundary values, $X_b(l = 0)$ and $X_b(l = L)$ were perturbed in the sense of Eq. (*7*) according to

$$X_b = X_{b,0} + K\,(X(x,t),\Phi(x)) \quad , \qquad (11)$$

where $X_{b,0}$ is a unperturbed boundary value of X under zero-derivative boundary conditions and K is the perturbation amplitude. At a value of $K = 7.0 \,.\, 10^{-3}$, the local control leads to simple periodic bulk oscillations of the entire system; any information about the spatial structure of the originally chaotic state, however, is lost.

We thank Prof. F. W. Schneider and Prof. M. Marek for helpful discussions. We further thank the Deutsche Forschungsgemeinschaft for financial support.

REFERENCES

1. Ott E., Grebogi C., Yorke J. A.: *Phys. Rev. Lett*. **1990**, *64*, 1196.
2. Hunt E. R.: *Phys. Rev. Lett*. **1991**, *67*, 1953.
3. Lekebusch A., Forster A., Schneider F. W.: *J. Phys. Chem*. **1995**, *99*, 681.
4. Pyragas K.: *Phys. Lett. A* **1992**, *170*, 421.
5. Kittel A., Parisi J., Pyragas K.: *Phys. Lett. A* **1995**, *198*, 433.
6. Lebender D., Muller J., Schneider F. W.: *J. Phys. Chem*. **1995**, *99*, 4992.
7. Kraus M., Muller J., Lebender D., Schneider F. W.: *Chem. Phys. Lett*. **1996**, *260*, 51.
8. Qin F., Wolf E. E.: *Chem. Eng. Sci*. **1995**, *50*, 117.

9. Fukunaga K.: *Introduction to Statistical Pattern Recognition*. Academic Press, New York 1990.
10. Graham M. D., Samuel L., Luss D.: *J. Phys. Chem*. **1993**, *97*, 889.
11. Quin F., Wolf E. E., Chang H. C.: *Phys. Rev. Lett*. **1994**, *72*, 1459.
12. Munster A. F., Hasal P., Snita D., Marek M.: *Phys. Rev. E: Stat. Phys., Plasmas, Fluids, Relat. Interdiscip. Top*. **1994**, *50*, 546.
13. Nandapurkar P. J., Hlavacek V., Van Rompay P.: *Chem. Eng. Sci*. **1986**, *41*, 2747.
14. Kuramoto Y.: *Prog. Theor. Phys*. **1978**, *64*, 346.
15. Chakravarti S., Marek M., Ray W. H.: *Phys. Rev. E: Stat. Phys., Plasmas, Fluids, Relat. Interdiscip. Top*. **1995**, *52*, 2407.
16. Marek M., Hasal P., Schreiber I., Munster A. F. in: *Fractals and Chaos in Chemical Engineering* (M. Giona and G. Biardi, Eds), p. 590. World Scientific, Singapore 1997.
17. Kolodner P., Slimani S., Aubry N., Lima R.: *Physica D (Amsterdam)* **1995**, *85*, 165.
18. Aubry N., Guyonnet R., Lima R.: *J. Stat. Phys*. **1991**, *63*, 683.